An Introduction to Hatsugai-Kohmoto Model and its physics

Zhiyan Wang[1]

[1]*Department of Physics, School of Science,*

Westlake University, Hangzhou 310030, China

(Dated: July 12, 2025)

Abstract: This work introduces the exactly solvable Hatsugai-Kohmoto (HK) model as a minimal platform for studying Mott physics, non-Fermi liquid behavior, and violations of Luttingers theorem. It shows how the HK model realizes a Mott insulating phase with emergent Luttinger surfaces, and how its metallic state lacks a conventional Fermi surface. Upon adding a superconducting pairing term, the model reveals unconventional superconducting features, such as spectral weight transfer and suppressed superfluid stiffness by mottness.

I. INTRODUCTION

A material's conductivity sets its role in electronic devices and transport. In conventional band theory, if electrons can be excited with gapless energy, the material is conductive. Conversely, if exciting charges requires overcoming a significant energy gap, the material behaves as an insulator. This theory successfully explains the fundamental differences between most metals and insulators: The Fermi level marks the dividing line for electron filling, and according to the Pauli exclusion principle, each momentum k can be occupied by two electrons with opposite spins – a state doubly occupancied. When the Fermi level lies within a partially filled conduction band, electrons can be excited to higher energy levels with infinitesimally small energy, making the material metallic. If all energy bands are either completely filled (requiring an energy gap for electron excitation) or completely empty (with no electrons to excite), the material acts as an insulator. This elegant theoretical framework, however, fails in the strong-correlation regime. Even when the electron filling is precisely half-filled, these materials stubbornly remain insulators. It strongly suggests that electron-electron interactions become dominant and can no longer be ignored.

This phenomenon is categorized under Mott physics. Specifically, due to Coulomb repulsion on the lattice, each site prefers to host only one electron. After half filling, any

electron movement would lead to a double occupancy, which is energetically forbidden. Consequently, all electrons are localized or, more precisely, charge frozen, turning the material into an insulator. Such an insulator, born from strong correlation effects, is called Mott insulator [1].

Beyond the Mott insulating state itself, the normal (non-superconducting) state of doped mott insulator displays a wide range of phenomena that defy Fermi liquid theorysuch as violations of Luttinger's theorem and the emergence of Fermi arcs. Adjacent to the pseudogap phase lies the so-called strange metal phase, which exhibits a linear-in-temperature resistivity, in stark contrast to the $\rho \propto T^2$ behavior expected from Fermi liquid theory. These anomalous phases together form an extensive region of non-Fermi liquid (NFL) behavior. Non-Fermi liquids have become a central focus in modern condensed matter physics, as they challenge the conventional quasiparticle framework and lack a well-defined Fermi surface. This has significant implications for our understanding of cuprates superconducting. In the search for minimal models that can faithfully capture such strong correlation effects and unconventional spectroscopic signatures, the Hubbard model once stood as a promising candidate. However, even the simplest single-band version of the Hubbard model remains analytically intractable, and theoretical progress has proven to be highly nontrivial.

Here, the Hatsugai-Kohmoto model (HK model) offers an exactly solvable pathway [2]. Its ground state inherently preserves the core physics of strong correlation effects, notably exhibiting a Mott phase. This not only aids in understanding both Mott insulators and the Hubbard model but also allows extensions of the HK model to analytically investigate Fermi arcs and non conventional superconducting.

II. HATSUGAI-KOHMOTO MODEL

The difficulties lie in strongly correlated systems is that low-energy system behavior cannot be described by single-particle ground states or perturbative methods, and mean-field theory can sometimes fall short. In this context, exactly solvable models play a role: though idealized, even unrealistic, they provide a controllable testing ground. The model designed by Hatsugai and Kohmoto was likely conceived with such considerations in mind. They constructed an interaction so specific that it no longer mixes different momenta (achieved through the conservation of center-of-mass momentum), thus completely decoupling the

entire many-body Hamiltonian in momentum space. Therefore, despite the infinite-range interaction not found in real materials employed by the HK model, it remains a powerful toy model. Its exact solvability and rich physical phenomena make it an important starting point for understanding certain non-perturbative behaviors.

The real-space Hamiltonian is given by:

$$\hat{H}_{\mathrm{HK}} = -t \sum_{\langle i,j\rangle,\sigma} c^{\dagger}_{i\sigma} c_{j\sigma} - \mu \sum_{j,\sigma} n_{j\sigma} + \frac{U}{N_s} \sum_{j_1+j_3=j_2+j_4} c^{\dagger}_{j_1\uparrow} c_{j_2\uparrow} c^{\dagger}_{j_3\downarrow} c_{j_4\downarrow}, \tag{1}$$

In this Hamiltonian, t denotes the nearest-neighbor hopping amplitude, and the first term describes the kinetic energy of electrons moving between adjacent lattice sites i and j. The index $\sigma = \uparrow, \downarrow$ labels the electron spin. The second term includes the chemical potential μ, controlling the electron density via the local number operator $n_{j\sigma} = c^{\dagger}_{j\sigma} c_{j\sigma}$. The third term encodes an interaction of strength U, which is nonlocal and acts between up-spin and down-spin electrons under the constraint that their total center-of-mass coordinate is conserved, i.e., only processes satisfying $j_1 + j_3 = j_2 + j_4$ contribute. The normalization by N_s, the total number of lattice sites, ensures extensivity of the interaction energy in the thermodynamic limit.

Upon Fourier transformation (detail is shown in Appendix), the Hamiltonian can be expressed in momentum space as:

$$\hat{H}_{\mathrm{HK}} = \sum_{k} \left[(\epsilon_k - \mu)(n_{k\uparrow} + n_{k\downarrow}) + U n_{k\uparrow} n_{k\downarrow} \right], \tag{2}$$

the Hamiltonian decouples into independent sectors labeled by momentum k. Each k-sector is a four-dimensional Hilbert space with basis states:

$$\{|0\rangle,\ c^{\dagger}_{k\uparrow}|0\rangle,\ c^{\dagger}_{k\downarrow}|0\rangle,\ c^{\dagger}_{k\uparrow} c^{\dagger}_{k\downarrow}|0\rangle\}, \tag{3}$$

and corresponding energies:

$$\begin{aligned} E_0 &= 0, \\ E_{\uparrow} &= \epsilon_k - \mu, \\ E_{\downarrow} &= \epsilon_k - \mu, \\ E_{\uparrow\downarrow} &= 2\epsilon_k - 2\mu + U. \end{aligned}$$

These four eigenstates have clear physical interpretations. The first eigenstate $|0\rangle$ corresponds to an empty occupancy at momentum k, with zero energy. The second and third

states, $c^\dagger_{k\uparrow}|0\rangle$ and $c^\dagger_{k\downarrow}|0\rangle$, represent singly occupied states with one spin-up or spin-down electron. They carry the same energy $\varepsilon_k - \mu$, reflecting the spin degeneracy of the system. The fourth state, $c^\dagger_{k\uparrow}c^\dagger_{k\downarrow}|0\rangle$, describes a doubly occupied state with both spin-up and spin-down electrons at the same momentum. Its energy is the sum of two single-particle contributions plus an additional interaction term U, accounting for the on-site repulsion between two electrons (here $U > 0$).

The crucial feature enabling exact solvability is that the Hamiltonian in momentum space becomes diagonal in momentum: it involves no scattering between different k values. The interaction term, $Un_{k\uparrow}n_{k\downarrow}$, is similar with the standard form of Hubbard interaction, but in momentum space. The Fourier-transformed Hubbard interaction $Un_{i\uparrow}n_{i\downarrow}$ in real space, which contains terms like $U\sum_{k,k',q} c^\dagger_{k-q,\uparrow}c_{k,\uparrow}c^\dagger_{k'+q,\downarrow}c_{k',\downarrow}$, involving momentum mixing across all sectors. In the HK model, the center-of-mass conserving structure of the interaction ensures that each momentum mode evolves independently, making the full many-body problem reducible to a product of local four-level systems.

A. Ground State

Because the Hamiltonian is a sum over decoupled k-sectors, the many-body ground state takes the product form:

$$|\Psi_{\text{gs}}\rangle = \bigotimes_k |\phi_k\rangle, \quad |\phi_k\rangle \in \{|0\rangle, |\uparrow\rangle, |\downarrow\rangle, |\uparrow\downarrow\rangle\}. \tag{4}$$

For each momentum k, the choice of $|\phi_k\rangle$ is determined by minimizing the corresponding energy among the three options:

- If $\epsilon_k - \mu > 0$, then $|0\rangle$ is the ground state: the site is empty.
- If $\epsilon_k - \mu < 0 < \epsilon_k - \mu + U$, then either $|\uparrow\rangle$ or $|\downarrow\rangle$ minimizes energy: the state is singly occupied.
- If $\epsilon_k - \mu + U < 0$, then $|\uparrow\downarrow\rangle$ is favored: the state is doubly occupied.

This segmentation in momentum space defines three regions determined by the value of μ relative to the dispersion ϵ_k and interaction U. Purely empty and doubly occupied states represent band insulators. The intermediate case is particularly noteworthy, where $\omega = 0$

falls entirely within the gap between the two bands. Considering the case where the gap U is very large, this will form a Mott insulator, because at this point, each momentum state can only be singly occupied, yet particles cannot move due to strong Coulomb repulsion. Naturally, in addition to these three states, the ground state itself can be a mixture, for instance, simultaneously exhibiting empty, doubly occupied, and singly occupied states. Hence, our next step is to determine the phase transition points between the Mott insulator and other phases.

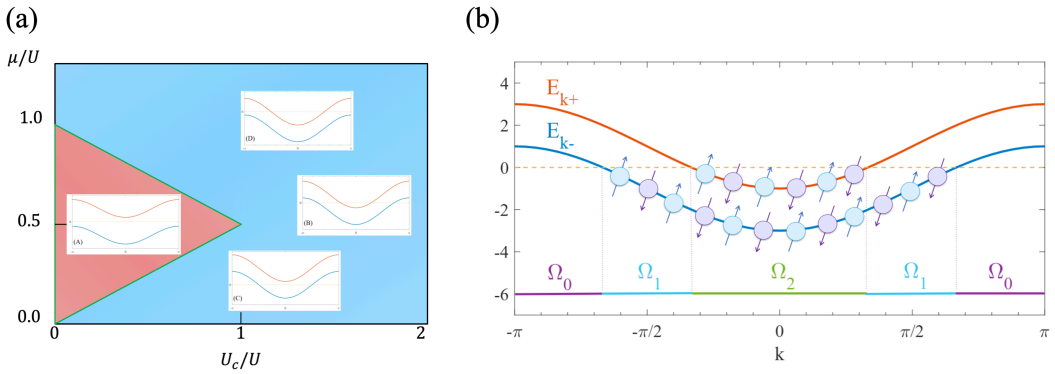

FIG. 1. Image modified from Ref. [3]. (a) The triangular region represents the Mott insulating phase, while the area outside this triangle corresponds to the metallic phase, as determined by Eq. 6. The inset illustrates the band structure for the corresponding parameters. (b) Schematic diagram of electron filling on the energy bands within the first Brillouin zone. The central Ω_2 region indicates double occupancy, where both bands fall below the Fermi level. The Ω_1 region represents single electron occupancy, where electrons can only fill the lower band. The outermost region corresponds to zero electron occupancy.

Consider a scenario where the system is currently in a Mott insulating state, with the system in a singly-occupied, degenerate ground state. It can be calculated that when an electron is added to the system, creating a doubly occupied site, the energy changes by: $\Delta E_k^+ = \epsilon_k - \mu + U$; and when an electron is removed from the system (or a hole is doped), the system's energy changes by: $\Delta E_k^- = -(\epsilon_k - \mu)$. For an insulator, the energy change should be larger than zero, regardless of whether an electron or a hole is doped. Therefore, two boundaries are defined by: $\Delta E_k^+ > 0$ and $\Delta E_k^- > 0$. Additionally, it should be noted that the non-interacting bandwidth is controled by the hopping strength, which is $W = 4td$, where d is the dimension. Consequently, $\epsilon_k \in [-W/2, W/2]$. Therefore, the boundaries are

defined as:

$$\epsilon_k^{min} = -W/2 > \mu - U, \epsilon_k^{max} = W/2 < \mu \tag{5}$$

Dividing both sides by U, to express them as ratios of parameters to the interaction strength:

$$\frac{\mu}{U} < 1 - \frac{W}{2U}, \quad \frac{\mu}{U} > \frac{W}{2U} \tag{6}$$

Combined with the non-hopping limit ($W/U = 0$), the triangular region enclosed by these two boundaries forms the Mott insulator phase, otherwise it is metallic. As shown in Fig 1, the closed region is determined dy $\frac{x}{2} < y < (1 - \frac{x}{2}), \quad x = 0$. And U_c in figure can be seen as W. For the half-filled case, where $\mu = U/2$, it can be determined that the **Metal-Mott phase transition occurs at** $U = W$. Evidently, even if the system is in a half-filled state, it does not necessarily imply it is a Mott insulator. When $U < W$, if the condition $\langle n_k \rangle = 1$ is still to be satisfied and the band crosses $\omega = 0$, it can only be a state where zero-, single-, and double-occupancy coexist. (If only the lower band crosses $\omega = 0$, this corresponds to $\langle n_k \rangle < 1$). The metallic state at half-filling can only exist if both the upper and lower bands partially cross $\omega = 0$. As U gradually increases towards $U > W$, the gap widens, and both bands shift away from $\omega = 0$.

III. NON-FERMI LIQUID AND LUTTINGER THEOREM

Luttinger's theorem is a core tenet of Fermi liquid theory, stating that the volume of the Fermi surface is directly proportional to the particle density. In Fermi liquid theory, the poles of the single-particle Green's function describe the quasi-particle dispersion relation, and a well-defined Fermi surface exists. At this Fermi surface, the momentum distribution function of particles exhibits a discontinuity, characterized by a finite quasiparticle weight Z_k. The generalized Luttinger's theorem, which describes the number of enclosed electrons within the Fermi surface, is given by the sign change of the Green's function as it crosses the Fermi surface:

$$2 \int d^d k \frac{1}{(2\pi)^d} \theta(G(k, \omega = 0)) = n \tag{7}$$

Here, the factor of 2 accounts for spin degeneracy, and d is dimension, n is the particle density in the system which is $n = N/V_{volume}$. In the process of adiabatically transforming

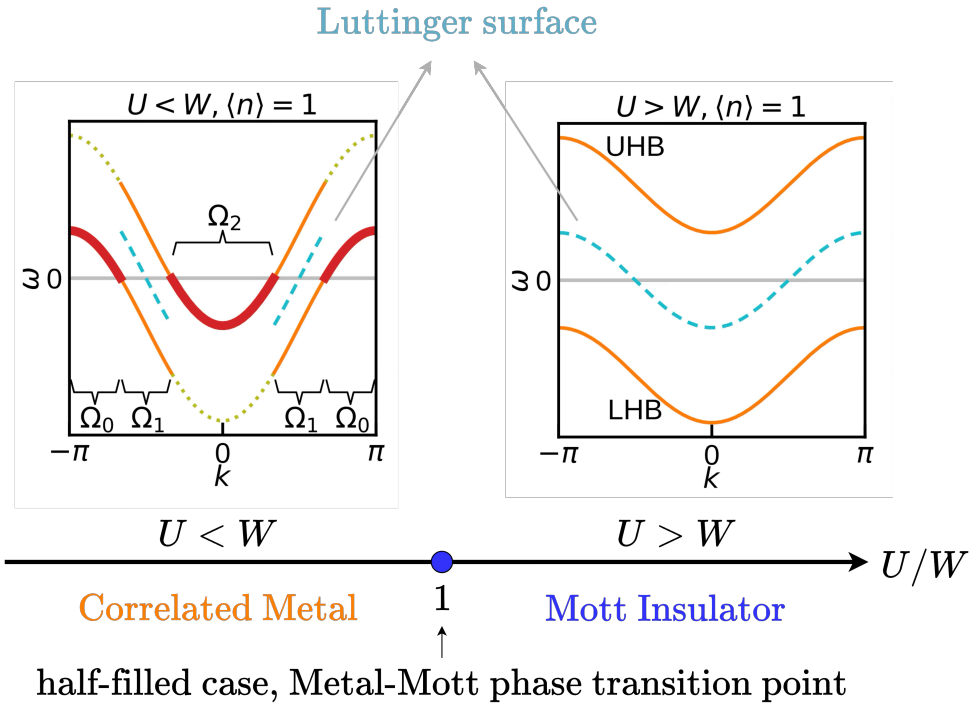

FIG. 2. Schematic band diagrams of the Hatsugai-Kohmoto (HK) model at half-filling, modified from Ref. [4]. (1) The Upper Hubbard Band (UHB) is represented by $\xi_k + U$, while the Lower Hubbard Band (LHB) is represented by ξ_k. At half-filling, the average occupation $\langle n_{k\sigma} \rangle = 1$, indicating that on average, each k-point is occupied by one electron. Ω_0, Ω_1, and Ω_2 denote the contributions from the empty, singly-occupied, and doubly-occupied regions, respectively. (2) Accordingly, their contributions to the spectral function of Eq. 9 are distinguished by different colors: a dashed line indicates zero contribution, an orange dashed line indicates a contribution of 1/2, and a thick red line indicates a contribution of 1. (3) The left side of the diagram represents the correlated metallic phase, while the right side represents the Mott insulating phase. The phase transition point occurs at $U = W$ (where W is the bandwidth). (4) It is also important to note that the light blue dashed line represents the Luttinger surface, which, by definition, is the zero surface of the real part of the Green's function contributed jointly by the upper and lower Hubbard bands in the singly-occupied region.

a free Fermi gas into a Fermi liquid, this relation does not change due to the introduction of weak interactions. This relationship, including the Fermi volume, remains unchanged when a free Fermi gas is adiabatically transformed into a Fermi liquid through the introduction of weak interactions. **However**, recent studies on strongly correlated systems, such as Mott insulators or pseudogap systems, suggest that this conventionally accepted theorem can be fundamentally violated. A hard LT violation specifically refers to scenarios where the above equation Eq. 7 is no longer satisfied. Some research indicates that this violation is caused by the presence of zeros in the Green's function. [4–8]

The zero-frequency Green's function may exhibit the following two forms of sign change: poles and zeros. In the case where only poles exist, LT performs well. But, once zeros appear, Eq. 7, which only counts the number of sign changes, will incorrectly count the zeros, ultimately leading to discrepancies with the actual number of particles. We will focus on the following questions:

1. How do zeros appear?
2. Why do zeros lead to the breakdown of LT?
3. Can such a breakdown be remedied, or what improvements can be made?

To answer the first question, we return to the main character of this paper, taking the HK model as an example. The retarded Green's function of the HK model is given by:

$$G^R_{k\sigma}(\omega) = \frac{1 - \langle \hat{n}_{k\sigma} \rangle}{\omega + \mu - \epsilon_k + i0^+} + \frac{\langle \hat{n}_{k\sigma} \rangle}{\omega + \mu - \epsilon_k - U + i0^+} \tag{8}$$

This is a two-pole structure. One pole, e.g., $\omega = -\mu + \epsilon_k$, where the Green's function diverges; the other is $\epsilon_k - \mu + U$. After separating the real and imaginary parts through $\frac{1}{x+i0^+} = \frac{1}{x} - i\pi\delta(x)$, the spectral function is given by:

$$A_{k\sigma}(\omega) = -\frac{1}{\pi}\mathrm{Im}G^R_{k\sigma}(\omega) = (1 - \langle \hat{n}_{k\sigma} \rangle)\delta(\omega - \epsilon_k + \mu) + \langle \hat{n}_{k\sigma} \rangle \delta(\omega - \epsilon_k + \mu - U) \tag{9}$$

These two spectral functions correspond to two distinct bands named Hubbard bands. The lower Hubbard band (LHB) corresponds to $\epsilon_k - \mu$, and the upper Hubbard band (UHB) corresponds to $\epsilon_k - \mu + U$ (where $U > 0$). When the average particle occupancy with determined k, σ is 1, meaning double occupancy, the first term vanishes. When the average particle occupancy is 0, the second term vanishes. For half-filling, $\langle \hat{n}_{k\sigma} \rangle = 1/2$, the two

spectral functions equally contribute to the total spectral function. In this case, the Green's function can be further simplified to:

$$G^R_{k\sigma}(\omega) = \frac{1}{\omega + i0^+ - (\xi_k + \frac{U}{2}) - \frac{(\frac{U}{2})^2}{\omega + i0^+ - (\xi_k + \frac{U}{2})}} \tag{10}$$

We can now observe that the two poles term have merged into one term. At the zero frequency $\omega = 0$, when $\xi_k = -U/2$, **the self-energy diverges**, which is defined as $\Sigma = \frac{(\frac{U}{2})^2}{\omega + i0^+ - (\xi_k + \frac{U}{2})}$. Considering the Kramers-Kronig relation, the real part of the Green's function can be completely expressed by imaginary part, which is:

$$\mathrm{Re}(G^R(\omega)) = -\frac{1}{\pi}\int_{-\infty}^{+\infty} \frac{\mathrm{Im}G^R(\omega')}{\omega - \omega'} d\omega' = \int_{-\infty}^{+\infty} \frac{A(\omega')}{\omega - \omega'} d\omega' \tag{11}$$

In this case, the lower and upper Hubbard bands jointly contribute to the real part of the Green's function. As seen from the front schematic of the half-filled conditions, this physical image can be summarized as follows: $k \in \Omega_1$ the singly occupied region, both the upper and lower Hubbard bands have contributions. At a given parameter point, such as when $2\xi_k + U = 0$, the real part of the Green's function exhibits a zero, and the self-energy diverges. This zero in the real part of the Green's function is defined as the Luttinger surface, represented by the blue line in the Fig. 2. Notably, the Luttinger surface appears exclusively in the singly occupied region.

So, why do zeros lead to the failure of Luttinger's theorem? Proving it is a bit tricky, but here may try to keep it simple. The whole story is about the Luttinger-Ward (LW) functional or self-energy function behavior. The LW functional basically bridges the Green's function and the free energy. We can then obtain the formula for the particle number density through the free energy. More specifically, the Luttinger integral I_L derived from the Green's function should consist of two integral terms:

$$I_L = I_1 + I_2 \tag{12}$$

$$I_1 = \frac{i}{2\pi}\int \frac{d^d\mathbf{k}}{(2\pi)^d} \oint_C d\omega \frac{\partial}{\partial\omega} \log(G(\mathbf{k},\omega)) = \frac{N}{2V}$$

$$I_2 = -i\int \frac{d^d\mathbf{k}}{(2\pi)^d} \oint_C \frac{d\omega}{2\pi} \left\{ G(\mathbf{k},\omega)\frac{\partial}{\partial\omega}\Sigma(\mathbf{k},\omega) \right\}$$

It can be proven that I_1 corresponds to Luttinger theorem, but the second term, I_2, involves the self-energy Σ. For systems where the Green's function possesses well-defined poles, it is

typically safe to calculated $I_2 = 0$ and thereby preserving Luttinger theorem. **In contrast**, as we mentioned earlier, the zero point of the Green's function, brings a trouble issue: the divergency of the self-energy Σ. At this point, the LW functional does not exist because it is unable to integral such divergency as in I_2, and thus $I_2 \neq 0$. Ultimately, this leads to Luttinger's integral $I_L \neq n$.

Interestingly, in certain cases, systems possessing **particle-hole symmetry (PHS)** might yield $I_2 = 0$, thus bringing us back to the Luttinger theorem. For instance, this occurs in the proof process for Luttinger liquids exhibiting PHS and satisfying Luttinger's theorem, or in the Hubbard model, where the satisfaction of LT requires the fine-tuned point to possess PHS. These observations might lead to a puzzling implication, prompting the question regarding the relationship between PHS and Luttinger's theorem: *Does Luttinger's theorem always hold in the presence of PHS?*. Certain topological approaches have rigorously demonstrated that PHS can be a sufficient condition for Luttinger's theorem to hold. For example, Seki and Yunoki [9] proposed a topological interpretation of the Luttinger theorem in which PHS ensures a quantized topological invariant associated with the Green's function, thereby guaranteeing the validity of LT. However, even when particle-hole symmetry does not exist, LT still holds. As the present work emphasizes, there exist counterexamples, supported in Refs. [10–14].

The relationship between PHS and LT.

While PHS can serve as a sufficient condition for Luttinger's theorem to hold, the converse does not apply. That is,

$$\text{PHS} \Rightarrow \text{LT holds} \quad \text{but} \quad \text{LT holds} \not\Rightarrow \text{PHS}$$

Therefore, the presence or absence of PHS should not be inferred solely from whether Luttingers theorem is satisfied.

Instead of focusing on symmetry-based heuristics, the present work arguesconsistent with Heath and Bedell [8]that the key to understanding the validity of Luttinger's theorem lies in the analytic structure of the self-energy $\Sigma(k, \omega)$, particularly its frequency dependence near $\omega = 0$.

The metallic ground state of the HK model violates Luttinger's Theorem, exhibiting

non-Fermi liquid behavior, except at PHS point. This holds true regardless of whether one considers the explicit self-energy divergence shown above, or follows the analysis of Ref. [3, 4, 15], which demonstrates that in both the HK model and its extensions, the Luttinger integral I_L differs from the particle density n.

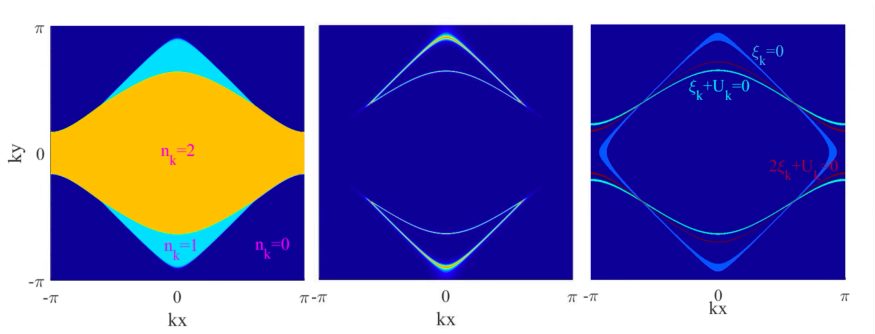

FIG. 3. Image taken from Ref. [3], (Left): Electron distribution function n_k, where the regions $n_k = 2$, $n_k = 1$, and $n_k = 0$ are clearly distinguished. (Middle): Spectral function $A(k, 0)$, showing the emergence of a Fermi arc. (Right): Contours corresponding to the conditions $\xi_k = 0$, $\xi_k + U_k = 0$, and $2\xi_k + U_k = 0$, which respectively represent the locations of the pseudo-Fermi surfaces and the Luttinger surface. Notably, the Luttinger surface intersects the pseudo-Fermi surface, truncating it and resulting in the appearance of a Fermi arc in the spectral function.

We now see how the presence of a Luttinger surface can fundamentally affect the structure of the Fermi surface and give rise to Fermi arcs. By further introducing a momentum-dependent interaction into the HK model, the interaction term becomes $U_k n_{k\uparrow} n_{k\downarrow}$, where U_k captures the momentum dependence of the interaction strength. As proposed in the work by Kun Yang et al. [16], this interaction takes the form

$$U_k = U - 2T_x \cos(k_x) - 2T_y \cos(k_y), \tag{13}$$

where T_x and T_y can be interpreted as effective hopping amplitudes in the x- and y-directions, respectively. This modification preserves the exactly solvable structure of the Green's function, which retains its two-pole form with the replacement $U \to U_k$:

$$G^R_{k\sigma}(\omega) = \frac{1 - \langle \hat{n}_{k\sigma} \rangle}{\omega + \mu - \epsilon_k + i0^+} + \frac{\langle \hat{n}_{k\sigma} \rangle}{\omega + \mu - \epsilon_k - U_k + i0^+}. \tag{14}$$

As before, one can define two types of surfaces: pseudo-Fermi surfaces, determined by the poles of the Greens function at $\omega = 0$, and the Luttinger surface, defined by the zero of the Greens function at $\omega = 0$.

The pseudo-Fermi surfaces are given by $\xi_k = 0$, marking the boundary between $n_k = 0$ and $n_k = 1$, and $\xi_k + U_k = 0$, separating $n_k = 1$ and $n_k = 2$. The Luttinger surface, however, is defined by the condition $2\xi_k + U_k = 0$. Once momentum anisotropy is introduced through the k-dependence of U_k, the Luttinger surface no longer simply lies outside or inside the pseudo-Fermi surfaceit can now intersect it at isolated points. As shown in Fig. 3, direct mechanism for the formation of Fermi arcs: **the Luttinger surface truncates the pseudo-Fermi surface**, leaving behind disconnected segments that appear as arcs in the spectral function.

IV. HK-BCS MODEL

The conventional BCS theory of superconductivity is deeply rooted in the framework of Fermi Liquid (FL) theory. In a Fermi liquid, low-energy excitations retain a one-to-one correspondence with free fermion states, albeit renormalized by interactionsmanifested through an effective mass and a well-defined quasiparticle residue. Importantly, this ensures the existence of a sharp Fermi surface, around which the concept of quasiparticles remains valid.

BCS theory builds upon this structure by postulating that an effective attractive interactiontypically mediated by phononsleads to the pairing of quasiparticles near the Fermi surface with opposite momenta and spins, forming Cooper pairs: $\hat{c}^\dagger_{k\sigma}\hat{c}^\dagger_{-k\sigma'}$. In the BCS ground state, the single-particle excitation spectrum develops an energy gap Δ_g, which leads to a universal ratio: $\frac{2\Delta_g}{k_B T_c} \approx 3.53$ is a constant. The excitations above the BCS ground state are normally described by Bogoliubov quasiparticles which are superpositions of electron and hole states.

This fundamental logic can be summarized as **FL** $\rightarrow$ **BCS**, and successfully applies to most conventional metals. **However**, for cuprates, the starting point of explanation is wrong. A crucial question now arises: how do we comprehend the superconducting instability of non-Fermi liquids (NFLs)? As pointed out by Phillips et al. [4], superconducting in cuprates do not originate from a Fermi liquid state, nor do they possess well-defined quasiparticles. Instead, they begin as a strongly correlated insulator and progressively evolve, through doping, into a state exhibiting superconducting phase. This pathway can be described as an unconventional **NFL** $\rightarrow$ **BCS** formation picture.

$$|\mathrm{GS}\rangle = \left(\prod_{k\in\Omega_2} c^\dagger_{k\uparrow}c^\dagger_{k\downarrow}\right)\left(\prod_{k\in\Omega_1} c^\dagger_{k\uparrow}|0\rangle\right) \tag{15}$$

To achieve this, the HK model itself is insufficient; it requires the additional incorporation of a superconducting pairing term. Here, we primarily discuss the work of Phillips and his group. They added an s-wave pairing term to the HK model:

$$H = H_{\mathrm{HK}} - gH_p, \quad H_p = \frac{1}{L^d}\hat{\Delta}^\dagger\hat{\Delta} \tag{16}$$

where $\hat{\Delta} = \sum_k b_k$ is the pairing annihilation operator, representing s-wave pairing with zero total momentum; $b_k = c_{k\downarrow}c_{-k\uparrow}$ is the operator that creates a pair, with electrons at k and $-k$ (where $k > 0$) having opposite spins. g is the pairing strength. This construction, similar to BCS pairing, is carried out in the HK metal (i.e., the NFL background).

First, a crucial question is whether such a construction leads to a superconducting instability. instability refers to the original system becoming unstable upon the addition of any attractive pairing interaction, subsequently flowing towards a superconducting state. Therefore, the binding energy E_b of the pair is calculated. $|\mathrm{GS}\rangle$ is a simplified form of an HK model ground state, incorporating mixtures of local, single-site, and double-occupancy states:

And we define $|\hat{\psi}\rangle = \sum_{k\in\Omega_0}\alpha_k b^\dagger_k|\mathrm{GS}\rangle$ as a state that produces a pairing in the ground state. The calculation results show that for any $g > 0$, bound-state energy $E < 0$, the system will flow towards the superconducting state. The next question is, how does this superconducting state differ from conventional FL-based superconductivity?

Phillips' group observed the phenomenon noted spectral weight transfer in the HK-BCS model that experimentally shown before. In the process of doping a Mott insulator, the weight in the electron spectral function shifts from the high-energy upper Hubbard band to the low-energy region, meaning the lower Hubbard band is enhanced while the upper Hubbard band is suppressed. Through calculations, they found that as the pairing interaction increases, the weight in the lower Hubbard band shows a clear upward trend.

This is attributed to the introduction of a pairing interaction in the HK model, which breaks the integrability of the kinetic and interaction terms. Originally, the single-particle excitations from the upper Hubbard band to doublons and from the lower Hubbard band to holons could be completely and well diagonalized within the HK Hamiltonian, but the

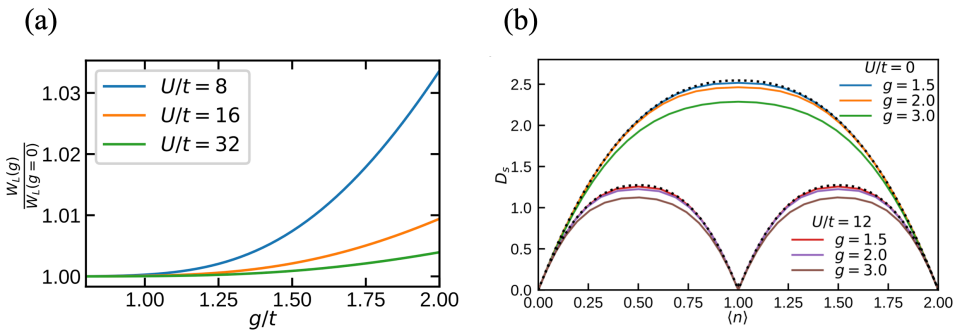

FIG. 4. Calculated results for the HK-BCS model, modified from Ref. [4]. (a) The calculated quantity is the ratio of the Lower Hubbard Band (LHB) weight to its weight without the attractive pairing potential g. This illustrates that as g increases, the relative weight of the LHB increases, indicating a transfer of spectral weight from high energies to low energies. (b) Superfluid stiffness is calculated and compared with the results of the conventional BCS model where the HK interaction is zero. It is observed that the results for the HK-BCS model exhibit a double-arched shape. The region where $\langle n \rangle = 2\langle n_{k\sigma} \rangle = 1$ corresponds to the half-filled Mott insulator, thus demonstrating that the superfluid stiffness is suppressed by the Mott side.

introduction of pairing breaks this integrability, leading to dynamic mixing between the Hubbard bands. The excitations are no longer traditional Bogoliubov quasiparticles, but rather a composite particle of upper and lower Hubbard band excitations.

Another notable difference is observed in superfluid stiffness or superconducting carrier density. The HK-BCS model predicts a significant suppression of superfluid density in the doped region near the Mott phase. The system exhibits a so-called double hump structure, where the superfluid density no longer increases monotonically with doping but reaches a peak near an optimal doping amount and then rapidly decreases on both sides. Conventional BCS theory struggles to explain this phenomenon, but the HK-BCS model, due to its non-Fermi liquid mechanism, or its naturally mottness, caputres this behavior so clear.

V. CONCLUSION AND DISCUSSION

The logic of this paper is grounded in the fact that the ground state of the HK model constitutes a non-Fermi liquid. In particular, motivated by the ideas and developments from the Phillips group, we examine how a superconducting state constructed on top of this

model exhibits several unconventional features beyond standard BCS theory. Accordingly, after presenting the metallic ground state of the HK model and confirming that it violates Luttingers theorem, we explore possible modifications to the HK model that give rise to Fermi arcs, as well as the emergence of unconventional superconductivity when an s-wave pairing term is introduced, following the Phillips group's approach. Due to space constraints, this work does not address the thermodynamic behavior of the HK model or earlier studies such as those on quantum oscillations. In short, the HK model still contains many intriguing physical features that remain to be introduced or explored.

1. **Absence of Long-Range Correlations:** Although not discussed in the main text, it has been shown in prior work that the HK model lacks long-range spin correlations in any spatial dimension. This sharply contrasts with the Hubbard model, which only loses long-range order in one dimension due to strong antiferromagnetic fluctuations. In $d \geq 2$, the strong-coupling limit of the Hubbard model maps onto an antiferromagnetic Heisenberg model, allowing for magnetic ordering even in the Mott insulating phase. However, does this necessarily imply that the Mott physics of the Hubbard model is fundamentally distinct from that of the HK model?

2. **On the contrary, the single-particle Greens functions of the HK and Hubbard models are remarkably similar.** The upper and lower Hubbard band structures and the presence of a Luttinger surface do not cease to exist in the absence of the full Hubbard Hamiltonian, and are instead manifestations of the underlying "Mottness." Furthermore, the spectral weight transfer phenomenon goes beyond the HK modelit is a universal signature of Mottness. Other works from the Phillips group have further argued that both models fall into the same high-temperature universality class. [17]

3. Z_2 **symmetry broken.** In their clarification of the relationship between the HK and Hubbard models, the Phillips group proposed that both models break a previously hidden symmetry. As early as 2000, P. W. Anderson and Haldane [18] had suggested that an $O(4)$ symmetry exists on the Fermi surface by treating charge degrees of freedom as a form of pseudospin. Specifically, the Fermi surface exhibits charge and spin conservation, corresponding to an $SU(2) \times SU(2)$ symmetry. However, this still lacks a hidden Z_2 symmetry that connects the $\det O(4) = \pm 1$ sectors. The full symmetry should be $O(4) \cong SU(2) \times SU(2) \times Z_2$, indicating that the spin and charge degrees of freedom are indistinguishable. Through their analysis, Phillips and collaborators [17] demonstrated that performing particle-hole conjuga-

tion on one spin species (while leaving the other unchanged) leaves the system invariantprovided this Z_2 symmetry is unbroken. However, both the HK and Hubbard models explicitly break this discrete symmetry. The result is a fundamental separation of spin and charge degrees of freedom, indicating that the transition from a Fermi liquid to a Mott insulator involves the breaking of a discrete Z_2 symmetry.

---

[1] N. F. MOTT, Metal-insulator transition, Rev. Mod. Phys. **40**, 677 (1968).

[2] Y. Hatsugai and M. Kohmoto, Exactly solvable model of correlated lattice electrons in any dimensions, Journal of the Physical Society of Japan **61**, 2056 (1992).

[3] M. Zhao, W.-W. Yang, and Y. Zhong, Hatsugai-kohmoto models: exactly solvable playground for mottness and non-fermi liquid, Journal of Physics: Condensed Matter **37**, 183005 (2025).

[4] P. W. Phillips, L. Yeo, and E. W. Huang, Exact superconducting instability in a doped mott insulator, arXiv: Superconductivity (2019).

[5] K. B. Dave, P. W. Phillips, and C. L. Kane, Absence of luttinger's theorem due to zeros in the single-particle green function, Phys. Rev. Lett. **110**, 090403 (2013).

[6] K. Limtragool, Z. Leong, and P. Phillips, Absence of luttinger's theorem for fermions with power-law green functions, SciPost Physics **5**, 10.21468/SciPostPhys.5.5.049 (2018).

[7] P. W. Phillips, Beyond particles: Unparticles in strongly correlated electron matter, arXiv: Strongly Correlated Electrons , 133 (2014).

[8] J. T. Heath and K. S. Bedell, Necessary and sufficient conditions for the validity of luttinger's theorem, New Journal of Physics **22**, 063011 (2020).

[9] K. Seki and S. Yunoki, Topological interpretation of the luttinger theorem, Phys. Rev. B **96**, 085124 (2017).

[10] K. B. Blagoev and K. S. Bedell, Luttinger's theorem and bosonization of the fermi surface, Physical Review Letters **79**, 1106 (1997).

[11] I. Dzyaloshinskii, Some consequences of the luttinger theorem: The luttinger surfaces in non-fermi liquids and mott insulators, Physical Review B **68**, 085113 (2003).

[12] A. Rosch, Breakdown of luttinger's theorem in two-dimensional non-fermi liquids, Physical Review Letters **90**, 076404 (2003).

[13] P. Nozières, On the luttinger theorem: Fermion density and zero-sound, Journal de Physique

I **7**, 701 (1997).

[14] M. P. Lilly *et al.*, Asymmetric spectral functions and fermi-liquid behavior, Physical Review B **53**, 13529 (1996).

[15] Y. Zhong, Solvable periodic anderson model with infinite-range hatsugai-kohmoto interaction: Ground-states and beyond, Phys. Rev. B **106**, 155119 (2022).

[16] K. Yang, Exactly solvable model of fermi arcs and pseudogap, Phys. Rev. B **103**, 024529 (2021).

[17] E. Huang, G. La Nave, and P. Phillips, Discrete symmetry breaking defines the mott quartic fixed point, Nature Physics **18** (2022).

[18] P. Anderson and F. Haldane, The symmetries of fermion fluids at low dimensions, Journal of Statistical Physics **103** (2000).

VI. APPENDIX

A. Hamiltonian of Hatsugai-Kohmoto model

Fourier transform using the standard convention:

$$c_n = \frac{1}{\sqrt{N_s}} \sum_k c_k e^{ikn}, \quad c_k = \frac{1}{\sqrt{N_s}} \sum_n c_n e^{-ikn}$$

We now perform the Fourier transform of the kinetic term in the Hubbard Hamiltonian. In real space, the hopping term reads:

$$H_t = -t \sum_{\langle i,j \rangle} c_i^\dagger c_j + \text{h.c.}$$

Substituting into the hopping term (for example, in one dimension):

$$H_t = -t \sum_n \left(\frac{1}{\sqrt{N_s}} \sum_k c_k^\dagger e^{-ikn} \right) \left(\frac{1}{\sqrt{N_s}} \sum_{k'} c_{k'} e^{ik'(n+1)} \right) + \text{h.c.}$$

$$= -t \sum_{k,k'} c_k^\dagger c_{k'} \left(\frac{1}{N_s} \sum_n e^{i(k'-k)n} \right) e^{ik'} + \text{h.c.}$$

Using the orthogonality relation:

$$\frac{1}{N} \sum_n e^{i(k'-k)n} = \delta_{k,k'}$$

we obtain:

$$H_t = -t \sum_k c_k^\dagger c_k e^{ik} + \text{h.c.} = -t \sum_k c_k^\dagger c_k \left(e^{ik} + e^{-ik} \right) = -2t \sum_k \cos(k)\, c_k^\dagger c_k$$

Here, in one dimension, the dispersion is $\epsilon_k = -2t\cos(k)$, in two dimension $\epsilon_k = -2t(\cos(k_x) + \cos(k_y))$ and so on. Chemical potential term is simple,

$$-\mu \sum_{j,\sigma} n_{j\sigma} = -\mu \sum_{j,\sigma} c_{j\sigma}^\dagger c_{j\sigma}$$

$$= -\mu \sum_\sigma \sum_j \left(\frac{1}{\sqrt{N_s}} \sum_{k'} e^{-ik'R_j} c_{k'\sigma}^\dagger \right) \left(\frac{1}{\sqrt{N_s}} \sum_k e^{ikR_j} c_{k\sigma} \right) = -\mu \sum_{k,\sigma} c_{k\sigma}^\dagger c_{k\sigma}$$

The interacting term:

$$\frac{U}{N_s^3}\sum_{k_1,k_2,k_3,k_4}\hat{c}^\dagger_{k_1\uparrow}\hat{c}_{k_2\uparrow}\hat{c}^\dagger_{k_3\downarrow}\hat{c}_{k_4\downarrow}\sum_{j_1,j_2,j_3,j_4}\delta_{j_1+j_3=j_2+j_4}e^{-i(k_1R_{j_1}+k_3R_{j_3})}e^{i(k_2R_{j_2}+k_4R_{j_4})}$$
$$=U\sum_{k_1,k_2,k_3,k_4}\hat{c}^\dagger_{k_1\uparrow}\hat{c}_{k_w2\uparrow}\hat{c}^\dagger_{k_3\downarrow}\hat{c}_{k_4\downarrow}\frac{1}{N_s}\sum_{j_1}e^{i(k_4-k_1)R_{j_1}}\frac{1}{N_s}\sum_{j_3}e^{i(k_4-k_3)R_{j_3}}\frac{1}{N_s}\sum_{j_2}e^{i(-k_4+k_2)R_{j_2}}$$
$$=U\sum_{k_1,k_2,k_3,k_4}\hat{c}^\dagger_{k_1\uparrow}\hat{c}_{k_2\uparrow}\hat{c}^\dagger_{k_3\downarrow}\hat{c}_{k_4\downarrow}\cdot\delta_{k_4,k_1}\delta_{k_4,k_3}\delta_{k_4,k_2}$$
$$=U\sum_k\hat{c}^\dagger_{k\uparrow}\hat{c}_{k\uparrow}\hat{c}^\dagger_{k\downarrow}\hat{c}_{k\downarrow}=U\sum_k\hat{n}_{k\uparrow}\hat{n}_{k\downarrow}$$

Therefore, the total Hamiltonian in momentum space is

$$\hat{H}_{\mathrm{HK}}=\sum_k\left[(\epsilon_k-\mu)(n_{k\uparrow}+n_{k\downarrow})+Un_{k\uparrow}n_{k\downarrow}\right]$$

B. Green's function

The retarded Green's function is defined as:

$$G^R(t)=-i\theta(t)\langle[\hat{A}(t),\hat{B}(0)]_\pm\rangle$$

or we expand it,

$$G(t)=-i\theta(t)\langle\hat{A}(t)\hat{B}(0)\pm\hat{B}(0)\hat{A}(t)\rangle$$

and this can be calculated by Lehmann representation. Notice $t\to\omega: G(\omega)=\int e^{i\omega t}G(t)dt$, so it gives,

$$G^R_{AB}(\omega)=\frac{1}{Z}\sum_{n,m}e^{-\beta E_n}\left[\frac{\langle n|\,\hat{A}\,|m\rangle\,\langle m|\,\hat{B}\,|n\rangle}{\omega+i0^+-(E_n-E_m)}\pm\frac{\langle n|\,\hat{B}\,|m\rangle\,\langle m|\,\hat{A}\,|n\rangle}{\omega+i0^+-(E_m-E_n)}\right]$$

In our main text, we used this form. Since spectral function is defined as

$$A(\omega)=-\frac{1}{\pi}\mathrm{Im}G(\omega)$$

Then separate real and imaginary parts by $\frac{1}{x+i0^+}=\frac{1}{x}-i\pi\delta(x)$, which gives,

$$A(\omega)=\frac{1}{Z}\sum_{n,m}e^{-\beta E_n}\cdot$$
$$\Big[\langle n|\,\hat{A}\,|m\rangle\,\langle m|\,\hat{B}\,|n\rangle\,\delta(\omega+E_n-E_m)$$
$$\pm\langle n|\,\hat{B}\,|m\rangle\,\langle m|\,\hat{A}\,|n\rangle\,\delta(\omega+E_m-E_n)\Big]$$

Through the equation of motion of the retarded Green's function,

$$\omega\langle\langle\hat{A}|\hat{B}\rangle\rangle_\omega = \langle[\hat{A},\hat{B}]_\pm\rangle + \langle\langle[\hat{A},\hat{H}]_-|\hat{B}\rangle\rangle_\omega$$

where the form $\langle\langle ...\rangle\rangle_\omega$ is like $\langle\langle\hat{A}|\hat{B}\rangle\rangle_\omega = \int e^{i\omega t}G(t)^R_{AB}dt = G(\omega)_{AB}$, The average value of the corresponding operators can be calculated:

$$\langle\hat{B}\hat{A}\rangle = \int_{-\infty}^{\infty} d\omega f_{F/B}(\omega)\left[-\frac{1}{\pi}\mathrm{Im}G^R_{AB}(\omega)\right]$$

where $f_{F/B}(\omega)$ is the Fermi-Dirac/Bose-Einstein distribution function.

Non-interacting Green's function

A simple example is when $\hat{A},\hat{B}$ is the field operator $\hat{\psi},\hat{\psi}^\dagger$ of fermion, so we can calculate non-interacting system Green's function:

$$H = \sum_{\mathbf{k}\sigma}(\epsilon_\mathbf{k}-\mu)\hat{\psi}^\dagger_{\mathbf{k}\sigma}\hat{\psi}_{\mathbf{k}\sigma}, \quad [\hat{\psi}_{\mathbf{k}\sigma},\hat{\psi}^\dagger_{\mathbf{k}'\sigma'}]_+ = \delta_{\mathbf{k},\mathbf{k}'}\delta_{\sigma,\sigma'}$$

because, $[A,BC] = B[A,C]+[A,B]C$, we can calculate:

$$\begin{aligned}
[\hat{\psi}_{\mathbf{k}\sigma},H]_- &= \left[\hat{\psi}_{\mathbf{k}\sigma},\sum_{\mathbf{k}'\sigma'}(\epsilon_{\mathbf{k}'}-\mu)\hat{\psi}^\dagger_{\mathbf{k}'\sigma'}\hat{\psi}_{\mathbf{k}'\sigma'}\right]_- \\
&= \sum(\epsilon_{\mathbf{k}'}-\mu)[\hat{\psi}_{\mathbf{k}\sigma},\hat{\psi}^\dagger_{\mathbf{k}'\sigma'}\hat{\psi}_{\mathbf{k}'\sigma'}]_- \\
&= (\epsilon_{\mathbf{k}'}-\mu)[\hat{\psi}_{\mathbf{k}\sigma},\hat{\psi}^\dagger_{\mathbf{k}'\sigma'}]_-\hat{\psi}_{\mathbf{k}'\sigma'} \\
&= (\epsilon_\mathbf{k}-\mu)\hat{\psi}_{\mathbf{k}\sigma}
\end{aligned}$$

where,

$$\begin{aligned}
[\hat{\psi}_{\mathbf{k}\sigma},\hat{\psi}^\dagger_{\mathbf{k}'\sigma'}]_-\hat{\psi}_{\mathbf{k}'\sigma'} &= [\hat{\psi}_{\mathbf{k}\sigma},\hat{\psi}^\dagger_{\mathbf{k}'\sigma'}]_+\hat{\psi}_{\mathbf{k}'\sigma'} - 2\hat{\psi}^\dagger_{\mathbf{k}'\sigma'}\hat{\psi}_{\mathbf{k}\sigma}\hat{\psi}_{\mathbf{k}'\sigma'} \\
&= \delta_{kk'\sigma\sigma'}\hat{\psi}_{\mathbf{k}'\sigma'} - 0 = \hat{\psi}_{\mathbf{k}\sigma}
\end{aligned}$$

thus,

$$\omega G_{\hat{\psi}\hat{\psi}^\dagger} = \langle[\hat{\psi},\hat{\psi}^\dagger]_+\rangle + G_{[\hat{\psi},H]_-,\hat{\psi}^\dagger} = \langle[\hat{\psi},\hat{\psi}^\dagger]_+\rangle + (\epsilon_\mathbf{k}-\mu)G_{\hat{\psi}\hat{\psi}^\dagger}$$

which gives single-particle Green's function of free fermion is $(\omega\to\omega+i0^+)$

$$G_{\hat{\psi},\hat{\psi}^\dagger}(\omega) = \frac{1}{\omega+i0^+-(\epsilon_\mathbf{k}-\mu)}$$

For interacting system, obtained by perturbative calculation, self-energy Σ is introduced:

$$G(\omega) = \frac{1}{\omega + i0^+ - \xi_k - \Sigma(k,\omega)}$$

where $\xi_k = \epsilon_{\mathbf{k}} - \mu$ is the non-interacting dispersion. Here we discuss how to obtain the single-particle Green's function of HK model.

Recall that $E_0 |0\rangle = 0, E_1 |1\rangle = \xi_k |1\rangle, E_2 |2\rangle = 2\xi_k + U |2\rangle$, let $\hat{A} = \hat{c}_{k,\sigma}\hat{B} = \hat{c}^\dagger_{k,\sigma}$, substitute into Lehmann representation. For example, when $|n\rangle = |0\rangle, |m\rangle = |1\rangle$, the term gives:

$$e^{-\beta E_0}\left(\frac{\langle 0|c_{k_\sigma}|1\rangle\langle 1|c^\dagger_{k_\sigma}|0\rangle}{\omega + i0^+ - \xi_k} + \frac{\langle 0|c^\dagger_{k_\sigma}|1\rangle\langle 1|c_{k_\sigma}|0\rangle}{\omega + i0^+ + \xi_k}\right)$$

we see the second term should vanish. Simmilarly, summing over all possible eigenstates with corresponding eigenvalues then we can obtain:

$$G(\omega) = \frac{1}{Z_k}\left[\left(1 + e^{-\beta\xi_k}\right)\frac{1}{\omega + i0^+ - \xi_k} + \left(e^{-\beta\xi_k} + e^{-\beta(2\xi_k+U)}\right)\frac{1}{\omega + i0^+ - (\xi_k + U)}\right]$$

Notice here we are still calcultating in one k-sector, so we don't want to calculate the total partition function which is $Z = \prod_k Z_k$.

$$Z_k = e^{-\beta H_k} = 1 + 2e^{-\beta\xi_k} + e^{-\beta(2\xi_k+U)} \quad 2 \text{ is degeneracy}$$

And also, we know that, according to $\langle \hat{c}^\dagger_{k\sigma}\hat{c}_{k\sigma}\rangle = \int_{-\infty}^{\infty} d\omega f_F(\omega)\left[-\frac{1}{\pi}\mathrm{Im}G(\omega)\right]$, it can be directly obtained by,

$$\langle \hat{n}_{k\sigma}\rangle = \frac{1}{Z_k}\left[\left(1 + e^{-\beta\xi_k}\right) f_F(\xi_k) + \left(e^{-\beta\xi_k} + e^{-\beta(2\xi_k+U)}\right) f_F(\xi_k + U)\right]$$

On the other hand, the average of $n_{k\sigma}$ can also be expressed as,

$$\langle n_{k\sigma}\rangle = \mathrm{Tr}\left[\hat{n}_{k\sigma}\, e^{-\beta\hat{H}_k}\right] = \sum_{\alpha\in\{0,\uparrow,\downarrow,\uparrow\downarrow\}} \langle\alpha|\hat{n}_{k\sigma}\, e^{-\beta\hat{H}_k}|\alpha\rangle = \sum_\alpha \langle\alpha|\hat{n}_{k\sigma}|\alpha\rangle \cdot e^{-\beta E_\alpha(k)}$$

Since $n_{k,\sigma}$ with a determined σ, the doubly occupancied state $|\uparrow\downarrow\rangle$ only contributes to $n_{k,\sigma} = 1$. So,

$$n_{k\sigma} = \frac{\mathrm{Tr}[\hat{n}_{k\sigma}e^{-\beta\hat{H}_k}]}{\mathcal{Z}_k} = \frac{e^{-\beta(\epsilon_{k\sigma}-\mu)} + e^{-\beta(2\epsilon_k - 2\mu + U)}}{1 + e^{-\beta(\epsilon_{k\uparrow}-\mu)} + e^{-\beta(\epsilon_{k\downarrow}-\mu)} + e^{-\beta(2\epsilon_k-2\mu+U)}} = \frac{e^{-\beta\xi_k} + e^{-\beta(2\xi_k+U)}}{Z_k}$$

Notice $1 + e^{-\beta\xi_k} = Z_k - e^{-\beta\xi_k} + e^{-\beta(2\xi_k+U)}$, in this way,

$$\langle n_{k\sigma}\rangle = (1 - \langle n_{k\sigma}\rangle)\, f_F(\xi_k) + \langle n_{k\sigma}\rangle f_F(\xi_k + U)$$

The Green's function is rewritten as:

$$G(\omega) = (1 - \langle n_{k\sigma}\rangle)\,\frac{1}{\omega + i0^+ - \xi_k} + \langle n_{k\sigma}\rangle \frac{1}{\omega + i0^+ - (\xi_k + U)}$$

which is same as Eq. 8 in our main text.

If Considering $T \to 0$, Direc-Fermi distribution goes to the step function. There are two jumps in electron distribution function which constructes to two quasi-fermi surface:

$$\langle \hat{n}_{k\sigma}\rangle = (1 - \langle n_{k\sigma}\rangle)\,\theta_1(-\xi_k) + \langle n_{k\sigma}\rangle \theta_2(-\xi_k - U)$$

where θ is the step function, only gives $\theta(x) = 0, 1$ when $x < 0, x > 0$.

The total electron density $n = 2n_{k\sigma}$, now we discuss,

1. $n_{k\sigma} = 1$ for $k < k_{F2}$,
2. $n_{k\sigma} = \frac{1}{2}$ for $k_{F2} < k < k_{F1}$,
3. $n_{k\sigma} = 0$ for $k > k_{F1}$.

Therefore, the electron density is calculated as:

$$n = 2\left[2\int_0^{k_{F2}} \frac{dk}{2\pi}\cdot 1 + 2\int_{k_{F2}}^{k_{F1}} \frac{dk}{2\pi}\cdot\frac{1}{2}\right] = 2\cdot\frac{k_{F1} + k_{F2}}{2\pi}$$

Here the factor of 2 accounts for spin degeneracy, and the expression shows that the total density depends on the average of the two pseudo-Fermi wavevectors.

Notice that, in the general case $\mu \neq U/2$, the two pseudo-Fermi momenta k_{F1} and k_{F2} are independently determined by $\xi_k = 0$ and $\xi_k + U = 0$ does not seem surprisingly indicating non-Fermi liquid behavior. **But**, at fine tuned point, which is as same as Hubbard model, when $\mu = U/2$, the system holds particle-hole symmetry (PHS). Under PHS ($\mu = U/2$), however, the condition $\xi_k = \epsilon_k - U/2$ enforces a symmetry between the two pseudo-Fermi surfaces. Recall that the dispersion gives that $k_F = \sqrt{\frac{2m}{\hbar^2}}$, then $k_{F2} = \sqrt{2m\mu}$ and $k_{F1} = \sqrt{2m(U-\mu)}$. Consequently:

$$n = 2\frac{k_{F1} + k_{F2}}{2\pi} = 2\frac{2k_F}{2\pi}, \quad \text{(PHS)}$$

which formally resembles the Luttinger theorem but with a critical distinction: k_F here represents an average of two correlated pseudo-Fermi surfaces rather than a single-particle Fermi momentum. This result doesnot deviate from the standard Luttinger theorem, which relates the electron density to a single Fermi surface volume $n_L = 2\cdot\frac{2k_F}{2\pi}$.

In our main text, half-filling condition is $\langle n_{k\sigma}\rangle = 1/2$, which leads to the following Green's function:

$$\begin{aligned}
G_{k\sigma}(\omega) &= \frac{1-\langle \hat{n}_{k\sigma}\rangle}{\omega+\mu-\epsilon_k+i0^+} + \frac{\langle \hat{n}_{k\sigma}\rangle}{\omega+\mu-\epsilon_k-U+i0^+} \\
&= \frac{\frac{1}{2}}{\omega-(\xi_k+\frac{U}{2})-\frac{U}{2}+i0^+} + \frac{\frac{1}{2}}{\omega-(\xi_k+\frac{U}{2})-\frac{U}{2}+i0^+} \\
&= \frac{1}{2}\left[\frac{1}{[\omega+i0^+-(\xi_k+\frac{U}{2})]+\frac{U}{2}} + \frac{1}{[\omega+i0^+-(\xi_k+\frac{U}{2})]-\frac{U}{2}}\right] \\
&= \frac{1}{2}\frac{2[\omega+i0^+-(\xi_k+\frac{U}{2})]}{[\omega+i0^+-(\xi_k+\frac{U}{2})]^2-(\frac{U}{2})^2} \\
&= \frac{1}{\omega+i0^+-(\xi_k+\frac{U}{2})-\frac{(\frac{U}{2})^2}{\omega+i0^+-(\xi_k+\frac{U}{2})}}
\end{aligned}$$

At zero frequency ($\omega = 0$), the single-particle Greens function $G(k,\omega)$ has a vanishing real part when $\xi_k = -U/2$, and this immediately implies a divergence of the self-energy $\Sigma(k,\omega)$ upon rewriting the expression in Dyson form. This observation plays a critical role in identifying singular behavior in the system.

C. Discussion

1. *PHS exists but LT broken?* Regarding the validity of Luttinger's theorem in Fermi liquids, we refer to Ref. [8], which provides a careful discussion on the relation between particle-hole symmetry (PHS) and Luttinger's theorem (LT). Interestingly, that work points out that LT can fail even in the presence of PHSas in superconducting statesand can hold in its absence. Their wording is: Considering that particle-hole symmetry is present in a superconducting state (where Luttinger's theorem clearly fails) yet is absent in certain Landau-Fermi liquids (where Luttinger's theorem clearly succeeds) ... This appears somewhat at odds with the conclusion in our main text, where we simply state that PHS has been shown to guarantee the validity of LT, while deliberately avoiding deeper discussion of exceptions. Given the lack of a comprehensive understanding, I regard the scenario in Ref. [8] as beyond the scope of the present work.

2. The most physically meaningful manifestation of PHS is the symmetry of the spectral function across $\omega = 0$, which corresponds to symmetry between electron and hole excitations.

However, the precise reason why this symmetry ensures the validity of Luttinger's theorem remains conceptually subtle and is still a subject of ongoing investigation. The proof by Seki and Yunoki [9] that PHS ensures the validity of Luttingers theorem still awaits careful examination by the present authors and should be distinguished from the scenarios discussed above.